



Unidirectional Seebeck effect in magnetic topological insulators

Xiao-Qin Yu ^{1,*}, Zhen-Gang Zhu ^{2,3,4,†} and Gang Su ^{3,4,5,‡}

¹*School of Physics and Electronics, Hunan University, Changsha 410082, China*

²*School of Electronic, Electrical, and Communication Engineering, University of Chinese Academy of Sciences, Beijing 100049, China*

³*Theoretical Condensed Matter Physics and Computational Materials Physics Laboratory, College of Physical Sciences, University of Chinese Academy of Sciences, Beijing 100049, China*

⁴*CAS Center for Excellence in Topological Quantum Computation, University of Chinese Academy of Sciences, Beijing 100190, China*

⁵*Kavli Institute for Theoretical Sciences, University of Chinese Academy of Sciences, Beijing 100190, China*



(Received 18 July 2019; revised manuscript received 14 October 2019; published 18 November 2019)

We theoretically investigate the temperature-gradient-dependent or unidirectional Seebeck effect (USE) in a magnetic/nonmagnetic topological insulator (TI) heterostructure with in-plane magnetization in terms of the semiclassical electron dynamics and Fermi golden rule. The USE has a quantum origin arising from the magnon asymmetric scattering of surface Dirac electrons on TI. We discuss the USE in the heterostructures, $\text{Cr}_x(\text{Bi}_{1-y}\text{Sb}_y)_{2-x}\text{Te}_3/(\text{Bi}_{1-y}\text{Sb}_y)_2\text{Te}_3$. The USE exhibits $\cos\phi$ dependence (measured from y direction) on the orientation of magnetization. It is found that the sign of USE stays unchanged when the system is transferred from p doping to n doping. The USE shows on inverse-linearly temperature dependent at high temperature.

DOI: [10.1103/PhysRevB.100.195418](https://doi.org/10.1103/PhysRevB.100.195418)

I. INTRODUCTION

The three-dimensional (3D) topological insulators (TI) [1,2] represent a new class of 3D materials with an insulating bulk and conductive surface states. The surface Dirac electrons have their spin locked to their momentum, namely, spin-momentum locking [Fig. 2(c)], hosting exotic topological quantum effects [3–6] and finding applications in spintronics and quantum computations. On the other hand, the interconversion of angular momentum between a conduction electron and local magnetization is one of the vital issues of contemporary spintronics research [7,8] and spin caloritronics [9–12]. Recently, the realization of a system in which spin-polarized two-dimensional (2D) Dirac electrons coexist with ferromagnetism on the surface of magnetic topological insulators (MTI) through doping magnetic impurities in TI [5,13] provides a new platform.

Owing to the interplay of the spin-momentum-locked surface states and magnetism, a series of novel transport phenomena are expected, such as quantum anomalous Hall effect (QAHE) [13], current-nonlinear Hall effect (CNHE) [14] and unidirectional magnetoresistance (UMR) [15–18]. UMR has recently been proposed in TI heterostructures [14,18–21] composed of nonmagnetic TI $(\text{Bi}_{1-y}\text{Sb}_y)_2\text{Te}_3$ (BST) [22] and magnetic TI $\text{Cr}_x(\text{Bi}_{1-y}\text{Sb}_y)_{2-x}\text{Te}_3$ (CBST) [23], which describes the resistance-value dependence on the sign of the outer product of current \mathbf{J} and the in-plane magnetization \mathbf{M} vectors and is identified to originate from the asymmetric scattering of electron by magnons [18]. It is natural to ask whether the Seebeck effect depends on the relative orientations of

the in-plane magnetization with respect to the temperature gradient in the heterostructures of BST/CBST.

In this paper, we theoretically investigate a temperature-gradient-direction-dependent or unidirectional Seebeck effect (USE) induced by magnon asymmetric scattering in the heterostructure of BST/CBST. We believe that the proposed effect is very useful in spin caloritronics. We derive the formula of nonlinear longitudinal current j_x response to the temperature gradient $\nabla_x T$ up to the second order based on the Boltzmann theory. We introduce, phenomenologically, a quantity ΔS which is expressed by the difference in Seebeck coefficients between the cases of the forward and backward temperature gradients ΔT [see Figs. 1(a) and 1(b)] to characterize the USE in Sec. II. We derive the formula of magnon relaxation time and determine the expressions of USE for BST/CBST heterostructure in Sec. III. The behavior of USE is discussed in Sec. IV.

II. UNIDIRECTIONAL SEEBECK EFFECT

With the relaxation time approximation, the Boltzmann equation for the distribution of electrons in absence of electric field reads [24,25]

$$f - f_0 = -\tau(\mathbf{k}) \frac{\partial f}{\partial r_a} \cdot v_a, \quad (1)$$

where τ represents the relaxation time, and v_a and r_a denote the a component of the velocity and coordinate position of electrons, respectively. f_0 is the local equilibrium distribution function. We are interested in the response up to the second order in temperature gradient and hence have the nonequilibrium distribution function $f \approx f_0 + f_1 + f_2$ with the term f_n to vanish as $(\partial T / \partial \mathbf{r}_a)^n$. After a series of careful derivations in Appendix A, the formulas of f_1 and f_2 can be determined and

*yuxiaoqin@hnu.edu.cn

†zgzh@ucas.ac.cn

‡gsu@ucas.ac.cn

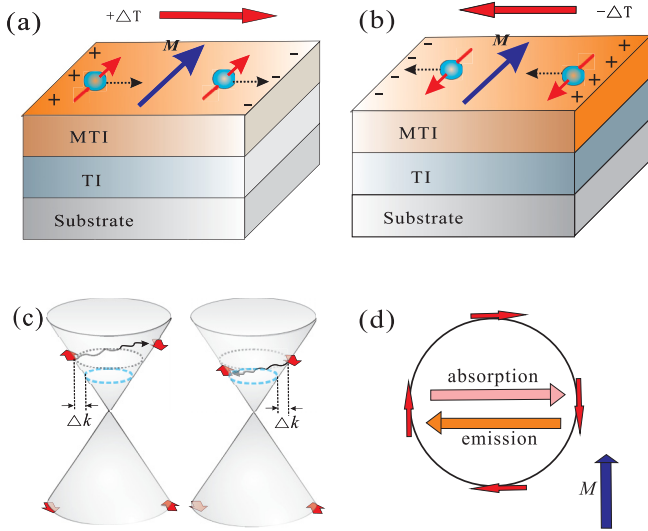


FIG. 1. Schematic illustration of the concept for USE in heterostructures topological insulator (TI)/magnetic TI under (a) $+\Delta T$ and (b) $-\Delta T$ temperature gradient. Here, the magnetic field, magnetization, and temperature gradient are all aligned in-plane. (c) Schematic illustration for the asymmetry magnon scattering of Dirac electrons on the spin-momentum-locked Fermi surface. (d) Top view of the scattering process for magnon emission and absorption.

are given in Eq. (A11). The charge current j_a in a direction is

$$j_a = -e \int [d\mathbf{k}] v_a f(\mathbf{r}, \mathbf{k}), \quad (2)$$

where $\int [d\mathbf{k}]$ is shorthand for $\int d\mathbf{k}/(2\pi)^2$. Based on Eqs. (2) and (A11), the current j_x in x direction is found to be

$$j_x = \alpha_{xx}^{(1)}(-\nabla_x T) + (\alpha_{xx,1}^{(2)} + \alpha_{xx,2}^{(2)})(\nabla_x T)^2 - \alpha_{xx,1}^{(2)} T \nabla_x^2 T, \quad (3)$$

with

$$\begin{aligned} \alpha_{xx}^{(1)} &= e \int [d\mathbf{k}] \tau(\mathbf{k}) v_x \frac{\epsilon_{\mathbf{k}} - \mu}{\hbar T} \frac{\partial f_0}{\partial k_x}, \\ \alpha_{xx,1}^{(2)} &= -e \int [d\mathbf{k}] (\tau(\mathbf{k}))^2 v_x^2 \frac{\epsilon_{\mathbf{k}} - \mu}{\hbar T^2} \frac{\partial f_0}{\partial k_x}, \\ \alpha_{xx,2}^{(2)} &= -e \int [d\mathbf{k}] (\tau(\mathbf{k}))^2 v_x \left(\frac{\epsilon_{\mathbf{k}} - \mu}{\hbar T} \right)^2 \frac{\partial^2 f_0}{\partial k_x^2}. \end{aligned} \quad (4)$$

Therefore, the relationship between temperature gradient and the thermoelectric voltage $\Delta V (= V_{\text{right}} - V_{\text{left}})$ can be expressed in a nonlinear form of

$$\Delta V = \frac{l}{\sigma_{xx}} [\alpha_{xx}^{(1)}(-\nabla_x T) + \alpha_{xx}^{(2)}(\nabla_x T)^2]. \quad (5)$$

To obtain Eq. (5), we have used $\Delta V = lE_x = j_x l / \sigma_{xx}$ and meanwhile assume the uniform temperature gradient in the system, i.e., $\nabla_x^2 T = 0$. Here $\alpha_{xx}^{(2)} = \alpha_{xx,1}^{(2)} + \alpha_{xx,2}^{(2)}$, and l is the length of the sample. Equation (5) hints that the voltage drop is nonlinearly dependent on the temperature gradient, which gives USE: when modulating the direction of temperature gradient, the voltage absolute value generated through the Seebeck effect is changed [Figs. 1(a) and 1(b)]. Therefore,

TABLE I. Parity about k_x for linear- k Dirac dispersion.

Function	Parity
$\epsilon_{\mathbf{k}}$	Even
v_x	Odd
$\frac{\partial f_0}{\partial k_x}$	Odd
$\frac{\partial^2 f_0}{\partial k_x^2}$	Even

the Seebeck coefficient $S = -(V_{\text{left}} - V_{\text{right}})/(T_{\text{left}} - T_{\text{right}})$, measured under plus or minus temperature difference ΔT [Figs. 1(a) and 1(b)], is noticeably distinguishing and is temperature-gradient-direction-dependent. Hence, the difference ΔS between the two temperature gradient directions can be applied to characterize the USE, which is determined by

$$\Delta S = S^+ - S^- = \frac{2\alpha_{xx}^{(2)} \Delta T}{\sigma_{xx} l}, \quad (6)$$

with $S^+ = \alpha_{xx}^{(1)}/\sigma_{xx} + \alpha_{xx}^{(2)} \Delta T / (l\sigma_{xx})$ and $S^- = \alpha_{xx}^{(1)}/\sigma_{xx} - \alpha_{xx}^{(2)} \Delta T / (l\sigma_{xx})$. Equation (6) indicates that ΔS is linearly proportional to the temperature gradient. Here we assume that the magnon scattering is completely independent of other scattering processes, such as the impurity, phonon, and so on. Thus, one could have

$$\frac{1}{\tau} = \frac{1}{\tau^0} + \frac{1}{\tau_{\text{mag}}}, \quad (7)$$

where τ^0 is the nonmagnetic scattering relaxation time and τ_{mag} is the scattered relaxation time by magnons. The impurity scattering is considered to be dominant here, which gives $\tau^0 \ll \tau_{\text{mag}}$. To first-order approximation, therefore, the relaxation time can be written as $\tau = \tau^0 - (\tau^0)^2 / \tau_{\text{mag}}$, leading to

$$\begin{aligned} \alpha_{xx}^{(2)} &= -e(\tau^0)^2 \int [d\mathbf{k}] \left\{ \left[v_x^2 \frac{\epsilon_{\mathbf{k}} - \epsilon_F}{\hbar T^2} \frac{\partial f_0}{\partial k_x} \right. \right. \\ &\quad \left. \left. + v_x \left(\frac{\epsilon_{\mathbf{k}} - \epsilon_F}{\hbar T} \right)^2 \frac{\partial^2 f_0}{\partial k_x^2} \right] - \frac{2\tau^0 v_x}{\tau_{\text{mag}}} \left[v_x \frac{\epsilon_{\mathbf{k}} - \epsilon_F}{\hbar T^2} \frac{\partial f_0}{\partial k_x} \right. \right. \\ &\quad \left. \left. + \left(\frac{\epsilon_{\mathbf{k}} - \epsilon_F}{\hbar T} \right)^2 \frac{\partial^2 f_0}{\partial k_x^2} \right] \right\}. \end{aligned} \quad (8)$$

Obviously, Eq. (8) involves two distinguished mechanisms that result in the nonlinear Seebeck effect and the USE: the asymmetric energy dispersion along k_x direction (the first term) and the asymmetric magnon scattering (the second term). In completely linear- k Dirac dispersion, one can actually find that the first term in Eq. (8) is zero by exploiting the parity (Table I). Besides, even in the presence of an in-plane magnetic field or magnetization, this term is still zero. This is because the Dirac point and the whole dispersion will shift in k space simultaneously and consistently [Fig. 2(c)] so that the velocity and the occupation are unchanged. In this work, we consider only the USE induced by the asymmetric magnon scattering, namely,

$$\begin{aligned} \alpha_{xx,\text{mag}}^{(2)} &= 2e(\tau^0)^3 \int [d\mathbf{k}] \frac{1}{\tau_{\text{mag}}(\mathbf{k})} \left[v_x^2 \frac{\epsilon_{\mathbf{k}} - \epsilon_F}{\hbar T^2} \frac{\partial f_0}{\partial k_x} \right. \\ &\quad \left. + v_x \left(\frac{\epsilon_{\mathbf{k}} - \epsilon_F}{\hbar T} \right)^2 \frac{\partial^2 f_0}{\partial k_x^2} \right]. \end{aligned} \quad (9)$$

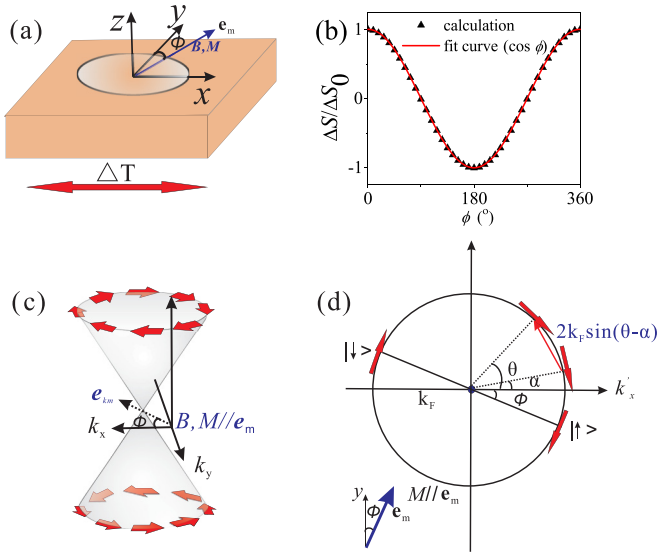


FIG. 2. (a) Schematic configuration for the measurement of in-plane magnetic field (or magnetization) ϕ dependence of ΔS , the azimuth angle ϕ is measured from the y axis. (b) The in-plane magnetization orientation (i.e., ϕ) dependence of normalized $\Delta S/\Delta S_0$. Here ΔS_0 is ΔS at $\phi = 0$. (c) Schematic diagram of the band structure under in-plane magnetization $M/e_m = (\sin \phi, \cos \phi)$ and spin-momentum locking of the surface Dirac state in TI. (d) Top view of the magnon scattering in 2D Dirac dispersion. The orientation of spin eigenfunctions $|\uparrow\rangle$ and $|\downarrow\rangle$ are illustrated when magnetization is parallel to e_m .

III. MODEL

One of candidate materials to observe the USE originating from the asymmetric scattering of electrons by magnons is the TI heterostructure BST/CBST. By tuning the composition y , one can modulate the Fermi energy E_f of the surface state inside the bulk band gap [14,18,20–22]. Hence, the carriers from the top and bottom surface states with a single Dirac cone will dominate the conduction. In addition, owing to the heterostructure, only one surface involved in the MTI layer interacts effectively with magnetic interaction [20,21]. Besides, the magnetization \mathbf{M} of CBST initially points along the z direction and leads to an exchange gap in the surface Dirac state. When the in-plane magnetic field B is applied up to B_0 (~ 0.7 T) [18], the orientation of magnetization will gradually be changed to the in-plane direction and the Dirac surface states will eventually become gapless. In this work, we consider the situation in which the magnetization is already oriented in-plane, with $\mathbf{M} = (m_x, m_y) = m\vec{e}_m$ and $\vec{e}_m = (\sin \phi, \cos \phi)$ [see Fig. 2(a)], where the azimuth angle ϕ is measured from the y axis. Owing to the coupling between the electron spin and localized magnetic moments, the Hamiltonian of the Dirac surface electrons is affected by the magnetization \mathbf{M} and can be written as

$$H_0 = (m \sin \phi + v_F \hbar k_y) \hat{\sigma}_x + (m \cos \phi - v_F \hbar k_x) \hat{\sigma}_y, \quad (10)$$

where v_F is the Fermi velocity, \hbar represents the Planck constant, $\hat{\sigma}$ denotes the Pauli matrices for the two basis functions of the energy band, m indicates the magnitude of

magnetization \mathbf{M} , and the definition of the azimuthal angle ϕ is given in Fig. 2(a). For simplicity, we also ignore the k^2 term and hexagonal warping (k^3 term) in the surface state of BST/CBST. The energy eigenvalues are

$$\epsilon_{\mathbf{k}} = n\sqrt{(v_F \hbar k_x - m \cos \phi)^2 + (v_F \hbar k_y + m \sin \phi)^2}, \quad (11)$$

where $n (= \pm 1)$ is the band index. Equation (11) hints that the Dirac point and the whole dispersion shifts towards the $\vec{e}_{k_m} = (\cos \phi, -\sin \phi)$ direction with the magnetic field or magnetization along direction \vec{e}_m [Figs. 2(a) and 2(c)]. In the following, we consider the interaction between the surface conduction electron and the localized spin composed of Cr d orbits. When \mathbf{M} is along the \vec{e}_m direction, the localized spin is pointing in the $-\vec{e}_m$ direction. Therefore, the angular momentum of the magnon is $+1$. Owing to the conservation of angular momentum, the interaction Hamiltonian H' is

$$\begin{aligned} H' &\approx \sum_i j_{\text{ex}} (c_{i,\uparrow}^+ c_{i,\downarrow} b_i + c_{i,\downarrow}^+ c_{i,\uparrow} b_i^+) \\ &= \sum_{\mathbf{k}\mathbf{q}} j_{\text{ex}} (c_{\mathbf{k}+\mathbf{q},\uparrow}^+ c_{\mathbf{k},\downarrow} b_{\mathbf{q}} + c_{\mathbf{k}-\mathbf{q},\downarrow}^+ c_{\mathbf{k},\uparrow} b_{\mathbf{q}}^+), \end{aligned} \quad (12)$$

where j_{ex} is the exchange-coupling constant, and b^+ (b) and c^+ (c) denote the creation (annihilation) operator of the magnon and surface Dirac electron, respectively. Equation (12) involves two processes: magnon absorption ($c_{\mathbf{k}+\mathbf{q},\uparrow}^+ c_{\mathbf{k},\downarrow} b_{\mathbf{q}}$) and magnon emission ($c_{\mathbf{k}-\mathbf{q},\downarrow}^+ c_{\mathbf{k},\uparrow} b_{\mathbf{q}}^+$). In the magnon absorption process, when the Dirac electron from the surface states $|\mathbf{k}, \downarrow\rangle$ is scattered to state $|\mathbf{k} + \mathbf{q}, \uparrow\rangle$, a magnon with momentum \mathbf{q} is absorbed due to the conservation of momentum and angular momentum [left plane of Fig. 1(c)]. In the magnon emission process, the electron spin is reversed from \uparrow ($s_\phi = 1/2$) to \downarrow ($s_\phi = -1/2$) by the emission of magnon [right plane of Fig. 1(c)] resulting from the spin-momentum locking of the surface Dirac state and the conservation of angular momentum.

Based on the Fermi golden rule, the magnon relaxation time τ_{mag} is found to be [14,18]

$$\frac{1}{\tau_{\text{mag}}(\mathbf{k})} \approx \sum_{\mathbf{k}'} W_{\text{mag}}(\mathbf{k}'|\mathbf{k}) [1 - f(\mathbf{k}')], \quad (13)$$

with

$$\begin{aligned} W_{\text{mag}}(\mathbf{k}'|\mathbf{k}) &= W_{\text{abs}}(\mathbf{k}', \sigma'; n_{\mathbf{k}'-\mathbf{k}} - 1 | \mathbf{k}, \sigma; n_{\mathbf{k}'-\mathbf{k}}) \\ &\quad + W_{\text{emit}}(\mathbf{k}', \sigma'; n_{\mathbf{k}-\mathbf{k}'} + 1 | \mathbf{k}, \sigma; n_{\mathbf{k}-\mathbf{k}'}), \end{aligned} \quad (14)$$

where $1 - f(\mathbf{k}')$ represents the probability of final state of the electron in which the electron is unoccupied. $n_{\mathbf{k}}$ denotes the number of magnons, W_{abs} (W_{emit}) are the scattering probabilities for the magnon absorption (emission) process, respectively, and are characterized as

$$\begin{aligned} W_{\text{abs}} &= \frac{2\pi}{\hbar} |\langle \mathbf{k}', \sigma'; n_{\mathbf{k}'-\mathbf{k}} - 1 | H' | \mathbf{k}, \sigma; n_{\mathbf{k}'-\mathbf{k}} \rangle|^2 \\ &\quad \times \delta(\epsilon_{\mathbf{k}'} - \epsilon_{\mathbf{k}} - \hbar\omega_{\mathbf{k}'-\mathbf{k}}), \end{aligned} \quad (15)$$

$$\begin{aligned} W_{\text{emit}} &= \frac{2\pi}{\hbar} |\langle \mathbf{k}', \sigma'; n_{\mathbf{k}-\mathbf{k}'} + 1 | H' | \mathbf{k}, \sigma; n_{\mathbf{k}-\mathbf{k}'} \rangle|^2 \\ &\quad \times \delta(\epsilon_{\mathbf{k}'} - \epsilon_{\mathbf{k}} + \hbar\omega_{\mathbf{k}-\mathbf{k}'}). \end{aligned}$$

Taking the interaction Hamiltonian H' [Eq. (12)] into Eq. (15), we have

$$W_{\text{abs}} = \frac{2\pi}{\hbar} j_{\text{ex}}^2 n_{\mathbf{k}-\mathbf{k}'} |\langle \sigma' | c_{\uparrow}^{\dagger} c_{\downarrow} | \sigma \rangle|^2 \delta(\epsilon_{\mathbf{k}'} - \epsilon_{\mathbf{k}} - \hbar\omega_{\mathbf{k}-\mathbf{k}'}),$$

$$W_{\text{emit}} = \frac{2\pi}{\hbar} j_{\text{ex}}^2 (n_{\mathbf{k}-\mathbf{k}'} + 1) |\langle \sigma' | c_{\downarrow}^{\dagger} c_{\uparrow} | \sigma \rangle|^2 \times \delta(\epsilon_{\mathbf{k}'} - \epsilon_{\mathbf{k}} - \hbar\omega_{\mathbf{k}-\mathbf{k}'}),$$
(16)

where $|\sigma\rangle(|\sigma'\rangle)$ indicates the initial (final) electron spin state, respectively. The spin orientation of surface electron in MTI around the Dirac cone is not fixed but rotates around the z axis [see Fig. 2(c)]. In the following, we consider the scattering from the position α to θ as shown in Fig. 2(d), namely, $|\sigma\rangle = |\alpha\rangle$ and $|\sigma'\rangle = |\theta\rangle$. Here, the spin eigenfunction at α (or θ) in $\{|\uparrow\rangle, |\downarrow\rangle\}$ representation is

$$|\alpha\rangle = \sin \frac{\phi + \alpha}{2} |\uparrow\rangle + \cos \frac{\phi + \alpha}{2} |\downarrow\rangle,$$

$$|\theta\rangle = \sin \frac{\phi + \theta}{2} |\uparrow\rangle + \cos \frac{\phi + \theta}{2} |\downarrow\rangle,$$
(17)

where $|\uparrow\rangle$ ($|\downarrow\rangle$) represents the state in which the spin direction is antiparallel (parallel) to the in-plane magnetic field, respectively. Therefore, taking the formulas of $|\sigma\rangle = |\alpha\rangle$ ($|\sigma'\rangle = |\theta\rangle$) determined by Eq. (17) into Eq. (16) and accompanied with a series of derivation in Appendix B, the magnon relaxation time in Eq. (13) is found to be

$$\frac{1}{\tau_{\text{mag}}(\alpha, \phi, \Delta k)} = \frac{1}{\tau_F^m} \int_0^{2\pi} d\theta V_{\text{mag}}(\theta + \phi, \alpha + \phi, \Delta k),$$
(18)

with $\frac{1}{\tau_F^m} = \frac{k_F}{(2\pi)} \frac{j_{\text{ex}}^2 A}{v_F \hbar^2}$, A is the area of the sample, and the integrand $V_{\text{mag}}(\theta, \alpha, \Delta k)$ is given in Eq. (B10).

IV. RESULTS AND DISCUSSION

By approximating the conductivity as $\sigma_{xx} \approx (e^2/4\pi\hbar)v_F k_F \tau^0$ [see Eq. (C5)], we found the quantity ΔS determining the USE in Eq. (6) to be (see details in Appendix C)

$$\frac{\Delta S}{\Delta T} = -\zeta \frac{A\epsilon_F}{IT} \iiint dx d\alpha d\theta V_{\text{mag}}\left(\theta + \phi, \alpha + \phi, \frac{k_B T x}{\hbar v_F}\right) \times \frac{x e^x \cos^3 \alpha}{(e^x + 1)^2} \left(1 + \frac{1 - e^x}{e^x + 1} x\right),$$
(19)

where $x = \hbar v_F \Delta k / (k_B T)$, with Δk measured from k_F (Fermi wave number). The typical scale $\zeta = 4k_B j_{\text{ex}}^2 (\tau^0)^2 / (e\hbar^3 v_F)$ is around $1.2 \times 10^9 [\text{eK m}]^{-1}$ for heterostructures BST/CBST. We use the following typical values: the Fermi velocity $v_F \approx 1 \times 10^5$ m/s [26], and the nonmagnetic scattering relaxation time $\tau^0 \approx 10^{-13}$ s estimated by $\tau^0 = \mu m / e$. Mobility μ of $(\text{Bi}_{1-x}\text{Sb}_x)_2\text{Te}_3$ ranges from 100 to 500 $\text{cm}^2 \text{V}^{-1} \text{s}^{-1}$ [22] when tuning the composition x . We use $\mu = 300 \text{ cm}^2 \text{V}^{-1} \text{s}^{-1}$ for an estimation. Although the value of the exchange-coupling energy j_{ex} is not well known for the heterostructures BST/CBST, here we adopt $j_{\text{ex}} \approx 0.1$ eV from Ref. [27], which is a typical value for exchange coupling of surface states Sb_2Te_3 and the magnetic impurities.

To disclose the microscopic origin of USE induced by magnon scattering intuitively, we first neglect the magnon

dispersion and use $g\mu_B B$ as a magnon energy [28] for simplicity. Thus, $\Delta S / \Delta T$ in Eq. (19) can be further simplified as (see details in Appendix C)

$$\frac{\Delta S}{\Delta T} = -\zeta \frac{3\pi A \tau_F^m \epsilon_F}{8IT} \cos \phi \int dx \left(\frac{1}{\tau^+} - \frac{1}{\tau^-} \right) \frac{x e^x}{(e^x + 1)^2} \times \left(1 + \frac{1 - e^x}{e^x + 1} x \right),$$
(20)

with

$$\frac{1}{\tau^+} = \frac{1}{e^{\beta\hbar\omega} - 1} \left(1 - \frac{1}{e^{(\alpha+\beta\hbar\omega)} + 1} \right) \frac{1}{\tau_F^m},$$
(21)

$$\frac{1}{\tau^-} = \left(\frac{1}{e^{\beta\hbar\omega} - 1} + 1 \right) \left(1 - \frac{1}{e^{(x-\beta\hbar\omega)} + 1} \right) \frac{1}{\tau_F^m}.$$
(22)

Here, τ^+ (τ^-) is the relaxation time of magnon scattering from the left (right) branch to the right (left) one [Fig. 1(d)]. The first factors of Eqs. (21) and (22) give the probability of magnon absorption and emission, respectively, and the second ones show the probability that the final state of the electrons is unoccupied.

Since $1/\tau^+$ and $1/\tau^-$ are not equal in general, Eq. (20) gives a finite USE, which is attributed to the magnon asymmetric scattering of electron in the TI, namely, the scattering rates are different in magnon absorption and emission processes. Equation (20) also hints that the in-plane magnetization directional dependence of normalized $\Delta S / \Delta S_0 \propto \cos \phi$, ΔS_0 is ΔS at $\phi = 0^\circ$. Thus, when the magnetization M is parallel or antiparallel to the y axis (i.e., $\phi = 0, \pi, 2\pi$), the $|\Delta S|$ will reach its maximum. However, the USE will disappear when magnetization is aligned to the direction of the temperature gradient (i.e., $M//x$). The $\cos \phi$ dependence on the orientation of magnetization of the USE can be ascribed to the asymmetric magnon scattering induced by the m_x ($\propto \cos \phi$) part of magnetization. The magnon scattering rate $1/\tau_{\text{mag}}$ can be divided into two parts: symmetric part $1/\tau_{\text{mag}}^S$ [Eq. (D2)] and antisymmetric part $1/\tau_{\text{mag}}^A$ [Eq. (D2)] when reversing k_x (a consequence of a mirror operation with respect to the $k_y - k_z$ plane in momentum space). m_x ($\propto \sin \phi$) (m_y) of magnetization only contributes to the symmetric (antisymmetric) scattering. Thus, only the antisymmetric part makes a contribution to the USE [see details in Appendix C]. Therefore, the USE shows $\cos \phi$ dependence on the orientation of magnetization.

In the following, we investigate the USE without neglecting the magnon band dispersion. In the long-wave-number case, the band dispersion of magnon is [29]

$$\hbar\omega = D_s q^2 + g\mu_B B$$

$$= 4D_s k_F^2 \sin^2(\theta - \alpha) + g\mu_B B,$$
(23)

where D_s is the spin stiffness constant, and $g \approx 2$ for the localized Cr moment in CBST. Figure 2 shows the in-plane magnetization orientation dependence of normalized ΔS ($\propto \cos \phi$) when considering the band dispersion of magnon. The result is consistent with the case in which the magnon dispersion is neglected. When the magnetic field or magnetization is aligned along the y direction, the signal of ΔS reaches the maximum.

Figure 3(a) shows the variation of ΔS with Fermi energy at different temperatures. The sign of ΔS does not change

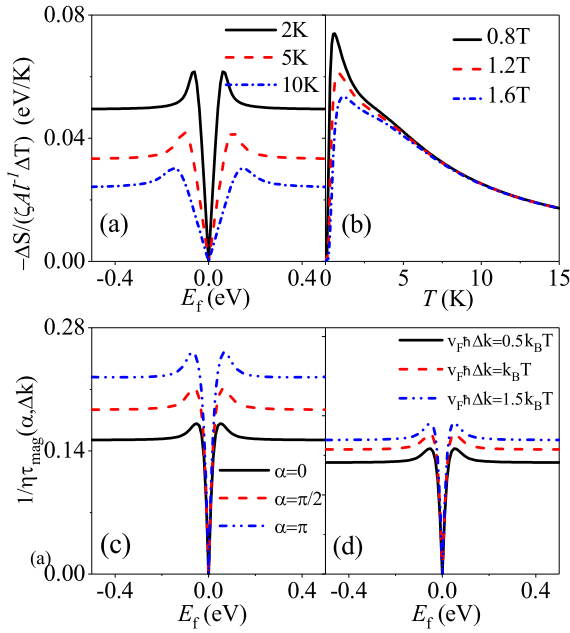


FIG. 3. (a) $\Delta S/\Delta T$ as a function of the Fermi energy for different temperature with the magnetic field $B = 1T$. (b) $\Delta S/\Delta T$ as a function of temperature gradient for different magnetic field. The magnetic field in (a) is taken at $1T$. The Fermi energy E_f is fixed at $0.1eV$ in (b). Magnon scattering rate $1/\eta\tau_{\text{mag}}(\alpha, \Delta k)$ as function of Fermi energy for different polar angle α in (c) and Δk in (d). α is polar angle measured from k_x axis and Δk is the radius measured from Fermi momentum k_F . Where $\eta = \epsilon_0 j_{\text{ex}}^2 A / (2\pi v_F^2 \hbar^3)$ with $\epsilon_0 = 1eV$ in (c)(d). The energy $v_F \hbar \Delta k$ is fixed at $1.5k_B T$ in (c) and $\alpha = 0$ in (d).

when the system is transferred from electron ($E_f < 0$) to hole ($E_f > 0$). This can be understood by considering the scattering process for holes in the same way as shown in Fig. 1(d) for electrons. With modulating the Fermi energy through gate voltage to the appropriate value (close to Dirac point), the signal of the unidirectional Seebeck effect ΔS can reach its maximum for both electrons and holes. The appearance of a peak in Fig. 3(a) can be qualitatively understood as follows: with increasing the absolute value of Fermi $|E_f|$, the energy of magnon contributing to the scattering processes increases so that the related magnon population decreases and the density of state of carriers (holes or electrons), on the contrary, increases. The combination of these two mechanisms leads to a magnon scattering rate $1/\tau_{\text{mag}}$ [Fig. 3(c)] that increases rapidly first and then gradually decreases due to the increase of magnon population, giving rise to a peak feature of $\Delta S/\Delta T$.

The temperature T dependence of ΔS at different magnetic fields is shown in Fig. 3(b). As expected, the unidirectional Seebeck effect tends to zero when T approaches zero owing to frozen magnon. Indeed, in the extremely low temperature regime $T \ll \hbar\omega_{\text{min}}$ ($\hbar\omega_{\text{max}} = g\mu_B B$), namely, $T \ll 1.34K$ for $B = 1T$, ΔS tends to zero owing to the frozen magnon. At the limit of high temperature $T \gg \hbar\omega_{\text{max}}$ ($\hbar\omega_{\text{max}} = 2D_s k_F^2 + g\mu_B B$ is the maximum energy of magnon), ΔS , as expected, varies inversely proportional with T . Therefore, a peak of ΔS will develop at finite temperature, and the peak shifts to higher

temperature with increasing the magnetic field. To understand the temperature dependence behaviors of the USE in high temperature qualitatively, we go back to the case in which the magnon dispersion is ignored for a more transparent picture. In the considered temperature regime, the number of magnons linearly depends on temperature ($n_B \approx k_B T / \hbar\omega$) and the difference between $1/[\exp(x + \beta\omega\hbar) + 1]$ and $1/[\exp(x - \beta\omega\hbar) + 1]$ is inversely dependent on T , leading to the temperature independence of $1/\tau^+ - 1/\tau^-$ in Eq. (20), giving rise to the inverse-linear temperature dependence of ΔS . Besides, the impact of varying magnetic field is also insignificant in this temperature regime.

To numerically estimate the proposed effect, we take $\Delta S/\zeta A l^{-1} \Delta T \approx 0.3 eV/K$ [Fig. 3(a)] for $T = 10K$. We also note that the USE in heterostructures BST/CBST can be estimated by the difference of voltage V_{USE} before and after reversing the direction of the temperature gradient as follows: $V_{\text{USE}} = |\Delta S \Delta T|$. The typical ζ in heterostructures BCT/CBST has been estimated to be of the order of $1.2 \times 10^9 [eK\text{m}]^{-1}$. Thus $V_{\text{USE}} \simeq 72 \text{ mV}$ with $\Delta T = 10\text{mK}$, and $w = A/l = 0.2 \mu\text{m}$ is the width of the sample, which is measurable [30].

V. CONCLUSION

In summary, we study the unidirectional Seebeck effect in the heterostructures of TI/MTI. It is found that Seebeck coefficient S is temperature-gradient-direction dependent and has a noticeable distinguishing feature when measured under positive ($+x$ axis) or negative ($-x$ axis) temperature difference ΔT . We have derived this difference $\Delta S = S^+ - S^-$ to characterize the unidirectional Seebeck effect induced by the magnon asymmetric scattering through the semiclassical framework of electron dynamics. Moreover, the quantity $\Delta S = S^+ - S^-$ is strongly dependent on the orientation of the in-plane magnetization. When the in-plane magnetic field or magnetization is vertical to the temperature gradient, $|\Delta S|$ reaches its maximum. However, the signal of ΔS will disappear when applying an magnetic field collinear to the temperature gradient. Fixing the magnetic field to the y direction, the unidirectional Seebeck effect is inverse-linearly dependent on temperature and insensitive to the magnetic field in the ‘‘high’’ temperature regime ($T \gg \hbar\omega_{\text{max}}$) in which T is far larger than the maximum energy of magnon contributing to scattering.

ACKNOWLEDGMENTS

This work is supported by the Fundamental Research Funds for the Central Universities and the NSFC (Grants No. 11674317 and No. 11974348). G.S. and Z.G.Z. are supported in part by the National Key R&D Program of China (Grant No. 2018FYA0305800), the Strategic Priority Research Program of CAS (Grant No. XDB28000000), the NSFC (Grant No. 11834014), and the Beijing Municipal Science and Technology Commission (Grant No. Z118100004218001).

APPENDIX A: THE NONEQUILIBRIUM DISTRIBUTION FUNCTION IN THE PRESENCE OF TEMPERATURE GRADIENT

With the relaxation time approximation, the Boltzmann equation for the distribution of electrons in absence of the electric field is

$$f - f_0 = -\tau \frac{\partial f}{\partial \mathbf{r}_a} \cdot \mathbf{v}_a. \quad (\text{A1})$$

To the response up to the second order in temperature gradient ∇T , the local distribution function $f(\mathbf{r}, \mathbf{k})$ is written as

$$\begin{aligned} f(\mathbf{k}, \mathbf{r}) &= f_0(\mathbf{k}, \mathbf{r}) + A_a \frac{\partial T}{\partial r_a} + B_{ab} \frac{\partial T}{\partial r_a} \frac{\partial T}{\partial r_b} + O[(\partial_a T)^3] \\ &= f_0(\mathbf{k}, \mathbf{r}) + f_1(\partial_a T) + f_2(\partial_a T \partial_b T) + O[(\partial_a T)^3], \end{aligned} \quad (\text{A2})$$

with

$$\begin{cases} f_1(\partial_a T) = A_a \partial_a T, \\ f_2(\partial_a T \partial_b T) = B_{ab} \partial_a T \partial_b T, \\ \partial_a \rightarrow \frac{\partial}{\partial r_a}, \end{cases} \quad (\text{A3})$$

where $f_0(\mathbf{k}, \mathbf{r})$ is the local equilibrium distribution function, which is itself fixed by the temperature at \mathbf{r} [31], giving rise to

$$\frac{\partial f_0}{\partial r_a} = \frac{\partial f_0}{\partial T} \frac{\partial T}{\partial r_a} \quad (\text{A4})$$

with

$$\frac{\partial f_0}{\partial T} = \frac{(\epsilon_{\mathbf{k}} - \mu)}{k_B T^2} (1 - f_0) f_0 = -\frac{(\epsilon_{\mathbf{k}} - \mu)}{T} \frac{\partial f_0}{\partial \epsilon_{\mathbf{k}}}. \quad (\text{A5})$$

By substituting the formula of f in Eq. (A2) into Eq. (1) and comparing the expansion coefficients in the first order of $\partial_a T$, one obtains

$$f_1(\partial_a T) = -\tau \frac{\partial f_0}{\partial r_a} \cdot \mathbf{v}_a + O[\partial_a T \partial_b T]. \quad (\text{A6})$$

Thus, we can have

$$f_1(\partial_a T) = -\tau \frac{\partial f_0}{\partial T} \partial_a T \cdot \mathbf{v}_a. \quad (\text{A7})$$

By iteration, then, we can have

$$\begin{aligned} f_2(\partial_a T \partial_b T) &= -\tau \frac{\partial f_1}{\partial r_a} \cdot \mathbf{v}_a \\ &= \tau^2 \left(\frac{\partial^2 f_0}{\partial T^2} \partial_a T \partial_b T + \frac{\partial f_0}{\partial T} \partial_{ab} T \right) v_b v_a. \end{aligned} \quad (\text{A8})$$

Here, we introduce a trick to transfer $\partial f_0 / \partial T$ into $\partial f_0 / \partial \mathbf{k}$ through a partial differential treatment

$$\frac{\partial f_0}{\partial \mathbf{k}} = \frac{\partial f_0}{\partial \epsilon_{\mathbf{k}}} \cdot \frac{\partial \epsilon_{\mathbf{k}}}{\partial \mathbf{k}} = -\frac{\partial f_0}{\partial T} \frac{\hbar \mathbf{v} T}{(\epsilon_{\mathbf{k}} - \mu)}. \quad (\text{A9})$$

In the above, we have used the relation $\frac{\partial f_0}{\partial T} = -\frac{(\epsilon_{\mathbf{k}} - \mu)}{T} \frac{\partial f_0}{\partial \epsilon_{\mathbf{k}}}$ [Eq. (A5)] and $\frac{\partial \epsilon_{\mathbf{k}}}{\partial \mathbf{k}} = \hbar \mathbf{v}$. From Eq. (A9), it is easy to obtain

the following identities:

$$\begin{aligned} \frac{\partial f_0}{\partial T} \cdot \mathbf{v}_a &= -\frac{\epsilon_{\mathbf{k}} - \mu}{\hbar T} \frac{\partial f_0}{\partial k_a}, \\ \frac{\partial^2 f_0}{\partial T^2} v_a v_b &= \frac{\epsilon_{\mathbf{k}} - \mu}{\hbar T^2} \frac{\partial f_0}{\partial k_a} v_b + \left(\frac{\epsilon_{\mathbf{k}} - \mu}{\hbar T} \right)^2 \frac{\partial^2 f_0}{\partial k_a \partial k_b}. \end{aligned} \quad (\text{A10})$$

By taking these identities into the formulas of f_1 [Eq. (A7)] and f_2 [Eq. (A8)], one obtains

$$\begin{aligned} f_1 &= \frac{\tau}{T \hbar} (\epsilon_{\mathbf{k}} - \mu) \frac{\partial f_0}{\partial k_a} \partial_a T, \\ f_2 &= -\frac{\tau^2}{T \hbar} (\epsilon_{\mathbf{k}} - \mu) v_b \frac{\partial f_0}{\partial k_a} \left(\partial_{ab} T - \frac{1}{T} \partial_a T \partial_b T \right) \\ &\quad + \frac{\tau^2}{\hbar^2 T^2} (\epsilon_{\mathbf{k}} - \mu)^2 \frac{\partial^2 f_0}{\partial k_a \partial k_b} \partial_a T \partial_b T. \end{aligned} \quad (\text{A11})$$

APPENDIX B: MAGNON RELAXATION TIME τ_{mag}

The magnon relaxation time τ_{mag} can be determined through Fermi golden rule given in Eq. (13). For simplicity, we divide τ_{mag} into

$$\frac{1}{\tau_{\text{mag}}(\mathbf{k})} = \frac{1}{\tau_{\text{mag}}^+(\mathbf{k})} + \frac{1}{\tau_{\text{mag}}^-(\mathbf{k})}, \quad (\text{B1})$$

with

$$\begin{aligned} \frac{1}{\tau_{\text{mag}}^+(\mathbf{k})} &= \sum_{\mathbf{k}'} W_{\text{abs}}(\mathbf{k}' | \mathbf{k}) [1 - f(\mathbf{k}')], \\ \frac{1}{\tau_{\text{mag}}^-(\mathbf{k})} &= \sum_{\mathbf{k}'} W_{\text{emit}}(\mathbf{k}' | \mathbf{k}) [1 - f(\mathbf{k}')], \end{aligned} \quad (\text{B2})$$

where W_{abs} and W_{emit} are given in Eq. (16). Substituting formulas of $|\sigma\rangle = |\alpha\rangle$ ($|\sigma'\rangle = |\theta\rangle$) determined by Eq. (17) into Eq. (16), we have

$$\begin{aligned} W_{\text{abs}} &= \frac{2\pi}{\hbar} j_{\text{ex}}^2 n_{\mathbf{k}'-\mathbf{k}} \cos^2 \frac{\alpha + \phi}{2} \sin^2 \frac{\theta + \phi}{2} \\ &\quad \times \delta(\epsilon_{\mathbf{k}'} - \epsilon_{\mathbf{k}} - \hbar \omega_{\mathbf{k}'-\mathbf{k}}), \\ W_{\text{emit}} &= \frac{2\pi}{\hbar} j_{\text{ex}}^2 (n_{\mathbf{k}-\mathbf{k}'} + 1) \sin^2 \frac{\alpha + \phi}{2} \cos^2 \frac{\theta + \phi}{2} \\ &\quad \times \delta(\epsilon_{\mathbf{k}'} - \epsilon_{\mathbf{k}} - \hbar \omega_{\mathbf{k}-\mathbf{k}'}). \end{aligned} \quad (\text{B3})$$

For a two-dimensional case, $\sum_{\mathbf{k}'} = \frac{A}{(2\pi)^2} \int d\mathbf{k}'$, where A is the area of the sample. Here we introduce a polar coordinate (α, k_1) in which the original point is located at the Dirac cone point, namely, $\mathbf{k}_0 = m(\cos \phi, -\sin \phi) / v_F \hbar$ [see Fig. 1(d)], yielding

$$\mathbf{k} = \left(k_1 \cos \alpha + \frac{m \cos \phi}{v_F \hbar}, k_1 \sin \alpha - \frac{m \sin \phi}{v_F \hbar} \right). \quad (\text{B4})$$

Thus, the energy eigenvalues in Eq. (11) and the integrated form of $d\mathbf{k}$ can be rewritten, respectively, as

$$\begin{aligned} \epsilon_{\mathbf{k}} &= \epsilon_{k_1} = n v_F \hbar k_1, \\ \epsilon_{\mathbf{k}} - \epsilon_F &= n v_F \hbar \Delta k, \\ \int d\mathbf{k} &\longrightarrow \int d\mathbf{k}_1 = \int d\alpha \int k_1 dk_1 \approx k_F \int d\alpha \int d\Delta k, \end{aligned} \quad (\text{B5})$$

where Δk is measured from k_F (Fermi wave number). In the following, we take the conduction band as an example, namely, $n = 1$, and consider the scattering from the position α to θ as shown in Fig. 2(d). Thus

$$\begin{aligned} \frac{1}{\tau_{\text{mag}}^+(\mathbf{k})} &= \frac{1}{\hbar} \frac{j_{\text{ex}}^2 A}{2\pi} k_F \int d\theta \int dk'_1 \cos^2 \frac{\alpha + \phi}{2} \sin^2 \frac{\theta + \phi}{2} \\ &\quad \times \frac{1}{\exp(\hbar\omega\beta) - 1} \left(1 - \frac{1}{\exp[\beta(v_F \hbar k'_1 - \epsilon_F)] + 1} \right) \\ &\quad \times \delta[v_F \hbar(k'_1 - k_1) - \hbar\omega] \\ &= \frac{1}{\tau_F^m} \int d\theta \frac{Q_{\text{mag}}^+(\Delta k_1)}{\exp(\hbar\omega\beta) - 1} \cos^2 \frac{\alpha + \phi}{2} \sin^2 \frac{\theta + \phi}{2}, \end{aligned} \quad (\text{B6})$$

with

$$\begin{aligned} Q_{\text{mag}}^+(\Delta k_1) &= \int dk'_1 \left(1 - \frac{1}{\exp[\beta(v_F \hbar k'_1 - \epsilon_F)] + 1} \right) \\ &\quad \times \delta\left(k'_1 - k_1 - \frac{\omega}{v_F}\right) \\ &= 1 - \frac{1}{\exp \beta[(\hbar\omega + \hbar v_F \Delta k)] + 1} \end{aligned} \quad (\text{B7})$$

and $\frac{1}{\tau_F^m} = \frac{k_F}{2\pi} \frac{j_{\text{ex}}^2 A}{v_F \hbar^2} \cdot \hbar\omega$ corresponds to the magnon energy with $2k_F \sin(\theta - \alpha)$ wave number. Similarly, one can have

$$\begin{aligned} \frac{1}{\tau_{\text{mag}}^-(\mathbf{k})} &= \frac{1}{\tau_F^m} \int_0^{2\pi} d\theta \sin^2 \frac{\phi + \alpha}{2} \cos^2 \frac{\phi + \theta}{2} \\ &\quad \times \left(\frac{1}{\exp(\hbar\omega\beta) - 1} + 1 \right) \frac{\exp \beta(\hbar v_F \Delta k - \hbar\omega)}{\exp \beta(\hbar v_F \Delta k - \hbar\omega) + 1}. \end{aligned} \quad (\text{B8})$$

Based on Eqs. (B1), (B7), and (B8), we obtain

$$\begin{aligned} \frac{1}{\tau_{\text{mag}}(\mathbf{k})} &= \frac{1}{\tau_{\text{mag}}(\alpha, \Delta k)} \\ &= \frac{1}{\tau_F^m} \int_0^{2\pi} d\theta V_{\text{mag}}(\theta + \phi, \alpha + \phi, \Delta k), \end{aligned} \quad (\text{B9})$$

with the integrand $V_{\text{mag}}(\theta + \phi, \alpha + \phi, \Delta k)$ defined as

$$\begin{aligned} V_{\text{mag}}(\theta + \phi, \alpha + \phi, \Delta k) &= \cos^2 \left(\frac{\alpha + \phi}{2} \right) \sin^2 \left(\frac{\theta + \phi}{2} \right) V_{\text{mag}}^+(\theta, \alpha, \Delta k) \\ &\quad + \sin^2 \left(\frac{\alpha + \phi}{2} \right) \cos^2 \left(\frac{\theta + \phi}{2} \right) V_{\text{mag}}^-(\theta, \alpha, \Delta k), \end{aligned} \quad (\text{B10})$$

where

$$\begin{aligned} V_{\text{mag}}^+(\theta, \alpha, \Delta k) &= \frac{1}{e^{\beta\hbar\omega} - 1} \left(1 - \frac{1}{e^{\beta(\hbar v_F \Delta k + \hbar\omega)} + 1} \right), \\ V_{\text{mag}}^-(\theta, \alpha, \Delta k) &= \left(1 - \frac{1}{e^{\beta(\hbar v_F \Delta k - \hbar\omega)} + 1} \right) \\ &\quad \times \left(\frac{1}{e^{\beta\hbar\omega} - 1} + 1 \right). \end{aligned} \quad (\text{B11})$$

APPENDIX C: THE FORMULA OF ΔS INDUCED BY THE MAGNON ASYMMETRY SCATTERING IN HETEROSTRUCTURES TI/MTI

Taking the magnetic relaxation time in Eq. (18) into Eq. (9), we can have $\alpha_{xx, \text{mag}}^{(2)}$ in polar coordinates ($\alpha, \Delta k$) (see Appendix B for detail), where α is the polar angle measured from k_x axis and Δk is the radius measured from k_F (Fermi momentum), as

$$\begin{aligned} \alpha_{xx, \text{mag}}^{(2)} &= \frac{2e(\tau^0)^3}{\tau_F^m} k_F \int d\Delta k \int d\alpha \int d\theta V_{\text{mag}} \\ &\quad \times (\theta + \phi, \alpha + \phi, \Delta k) \\ &\quad \times \left[v_x^2 \frac{v_F \Delta k}{T^2} \frac{\partial f_0}{\partial k_x} + v_x \left(\frac{v_F \Delta k}{T} \right)^2 \frac{\partial^2 f_0}{\partial^2 k_x} \right]. \end{aligned} \quad (\text{C1})$$

For $v_x(\mathbf{k})$,

$$v_x = \frac{1}{\hbar} \frac{\partial \epsilon_{\mathbf{k}}}{\partial k_x} = v_F \cos \alpha. \quad (\text{C2})$$

For $\frac{\partial f_0}{\partial k_x}$,

$$\frac{\partial f_0}{\partial k_x}(\alpha, \Delta k) = -\frac{P}{(P+1)^2} \beta v_F \hbar \cos \alpha. \quad (\text{C3})$$

For $\frac{\partial^2 f_0}{\partial k_x^2}$,

$$\begin{aligned} \frac{\partial^2 f_0}{\partial k_x^2}(\alpha, \Delta k) &= -\frac{\beta \hbar v_F}{k_F} \frac{P}{(P+1)^2} \sin^2 \alpha + (\beta \hbar v_F)^2 \cos^2 \alpha \\ &\quad \times \frac{P(P-1)}{(P+1)^3} \\ &\approx (\beta \hbar v_F)^2 \frac{P(P-1)}{(P+1)^3} \cos^2 \alpha, \end{aligned} \quad (\text{C4})$$

with $P = e^{\beta \hbar v_F \Delta k}$. Here, in the third line of Eq. (C4), we can ignore the first term since $\beta \hbar v_F k_F \gg 1$ except for the immediate vicinity of the Dirac point. Meanwhile,

$$\begin{aligned} \sigma_{xx} &= -\frac{e^2}{\hbar} \frac{1}{(2\pi)^2} \int d\mathbf{k} \tau(\mathbf{k}) v_x(\mathbf{k}) \frac{\partial f}{\partial k_x} \\ &\approx -\frac{e^2}{\hbar} \frac{\tau^0 k_F}{(2\pi)^2} \int d\Delta k \int_0^{2\pi} d\alpha v_x(\alpha) \frac{\partial f}{\partial k_x}(\Delta k, \alpha) \\ &= \frac{e^2}{4\pi \hbar} v_F k_F \tau^0. \end{aligned} \quad (\text{C5})$$

Therefore, from Eq. (6) we can determine the expression of ΔS for characterizing the USE as

$$\begin{aligned} \Delta S &= -\zeta \frac{A \epsilon_F \Delta T}{lT} \int d\Delta k \int d\alpha \int d\theta V_{\text{mag}}(\theta + \phi, \alpha + \phi, \Delta k) \\ &\quad \times \left(\frac{\hbar v_F}{k_B T} \right)^2 \Delta k \frac{P \cos^3 \alpha}{(P+1)^2} \left(1 + \frac{1-P}{P+1} \frac{\hbar v_F \Delta k}{k_B T} \right), \end{aligned} \quad (\text{C6})$$

where $\zeta = 4k_B j_{\text{ex}}^2 (\tau^0)^2 / (e \hbar^3 v_F)$. Let $x = \hbar v_F \Delta k / (k_B T)$ in Eq. (C6), and taking the formula of $P = e^{\hbar v_F \Delta k / (k_B T)}$ into it, we have obtained the expression of ΔS in Eq. (19) in the main text. In the following, we consider a situation in which we neglect magnon dispersion and use $g\mu_B B$ as magnon energy, namely, $\hbar\omega = g\mu_B B$. Thus, $V_{\text{mag}}^{+(-)}(\theta, \alpha, \Delta k)$ in Eq. (B11) will

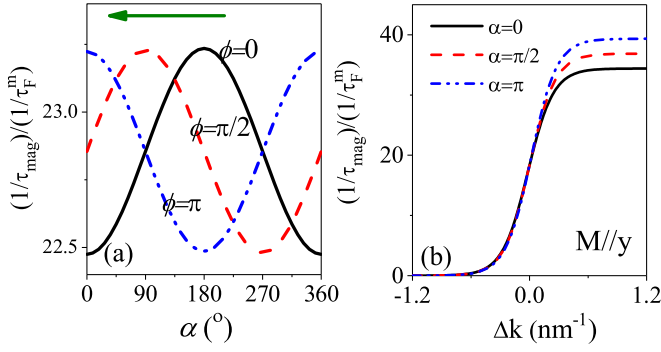


FIG. 4. α dependence of $1/\tau_{\text{mag}}$ for different ϕ is shown in (a) and Δk dependence of $1/\tau_{\text{mag}}$ for different polar angle α is shown in (b) with magnetization along y direction, namely $\phi = 0$. The magnetic field is $B = 1$ T and the temperature is $T=10$ K. α is polar angle measured from k_x axis and Δk is the radius measured from Fermi momentum k_F . The azimuth angle ϕ is used to indicate the magnetization orientation measured from the y axis.

be independent of θ and α , and thus we rewrite them as $V_{\text{mag}}^{+(-)}(\Delta k)$. Therefore the integration of the angle-dependent part in Eq. (C6) is found to be

$$\begin{aligned} \Xi &= \int_0^{2\pi} d\alpha \int_0^{2\pi} d\theta V_{\text{mag}}(\theta + \phi, \alpha + \phi, \Delta k) \cos^3 \alpha \\ &= \int_0^{2\pi} d\alpha \int_0^{2\pi} d\theta \cos^3 \alpha \left[\cos^2 \frac{\phi + \alpha}{2} \sin^2 \left(\frac{\phi + \theta}{2} \right) \right. \\ &\quad \times V_{\text{mag}}^+(\Delta k) + \sin^2 \frac{\phi + \alpha}{2} \cos^2 \left(\frac{\phi + \theta}{2} \right) V_{\text{mag}}^-(\Delta k) \left. \right] \\ &= \frac{3\pi^2}{8} [V_{\text{mag}}^+(\Delta k) - V_{\text{mag}}^-(\Delta k)] \cos \phi. \end{aligned} \quad (\text{C7})$$

Thus

$$\begin{aligned} \frac{\Delta S}{\Delta T} &= -\zeta \frac{3\pi^2 A l \epsilon_F \Delta T}{8T} \cos \phi \int d\Delta k [V_{\text{mag}}^+(\Delta k) - V_{\text{mag}}^-(\Delta k)] \\ &\quad \times \left(\frac{\hbar v_F}{k_B T} \right)^2 \Delta k \frac{P \cos^3 \alpha}{(P+1)^2} \left(1 + \frac{1-P}{P+1} \frac{\hbar v_F \Delta k}{k_B T} \right) \\ &= \zeta \frac{3\pi^2 A l \tau_F^m \epsilon_F \Delta T}{8T} \cos \phi \int dx \left(\frac{1}{\tau^+} - \frac{1}{\tau^-} \right) \\ &\quad \times \frac{x e^x}{(1+e^x)^2} \left(1 + \frac{1-e^x}{e^x+1} x \right). \end{aligned} \quad (\text{C8})$$

To obtain the third line, we have make use of $x = \hbar v_F \Delta k / (k_B T)$ and $1/\tau^{+(-)} = V_{\text{mag}}^{+(-)} / \tau_F^m$ given in Eqs. (21) and (22).

APPENDIX D: THE ANALYSIS OF SYMMETRIES (OR PARTIES) OF $1/\tau_{\text{mag}}$ AND THE $\cos \phi$ DEPENDENCE OF MAGNETIZATION OF USE

In this Appendix, the symmetries (or parties) of $1/\tau_{\text{mag}}$ and the $\cos \phi$ dependence of $\Delta S / \Delta T$ in Eq. (20) will be analyzed. Before a detailed analysis, we would like to introduce two concepts: (1) It is noted that the symmetry/antisymmetry of a function $f(k_x, k_y)$ corresponds to even/odd parties with

respect to k_x , respectively, namely, $f(k_x, k_y) = f(-k_x, k_y) / f(k_x, k_y) = -f(-k_x, k_y)$. This is a consequence of mirror symmetry with respect to the k_y - k_z plane in momentum space. (2) In polar coordinate $(\alpha, \Delta k)$, where α is the polar angle measured from the k_x axis and Δk is the radius measured from the Fermi momentum k_F , $\cos \alpha$ ($\sin \alpha$) dependence of function f represents that f is odd (even) function with respect to k_x , respectively.

To understand how the $\cos \phi$ dependence of $\Delta S / \Delta T$ in Eq. (20) appears physically, we can investigate the symmetry of magnon scattering time with respect to k_x . As mentioned above Eq. (C7), when neglecting magnon dispersion and using $g u_B B$ as magnon energy, $V_{\text{mag}}^{+(-)}(\theta, \alpha, \Delta k)$ in Eq. (B11) will be independent of θ and α and is rewritten as $V_{\text{mag}}^{+(-)}(\Delta k)$. Hence, the magnon scattering time τ_{mag} in Eq. (B9) is found to be

$$\begin{aligned} \frac{1}{\tau_{\text{mag}}(\alpha, \Delta k)} &= \int_0^{2\pi} \frac{d\theta}{\tau_F^m} V_{\text{mag}}(\theta + \phi, \alpha + \phi, \Delta k) \\ &= \int_0^{2\pi} \frac{d\theta}{\tau_F^m} \left[\cos^2 \frac{\phi + \alpha}{2} \sin^2 \left(\frac{\phi + \theta}{2} \right) V_{\text{mag}}^+(\Delta k) \right. \\ &\quad \left. + \sin^2 \frac{\phi + \alpha}{2} \cos^2 \left(\frac{\phi + \theta}{2} \right) V_{\text{mag}}^-(\Delta k) \right] \\ &= \frac{1}{\tau_{\text{mag}}^S} + \frac{1}{\tau_{\text{mag}}^A}, \end{aligned} \quad (\text{D1})$$

with

$$\begin{aligned} \frac{1}{\tau_{\text{mag}}^S} &= \frac{\pi}{2\tau_F^m} [(V_{\text{mag}}^+(\Delta k) + V_{\text{mag}}^-(\Delta k)) \\ &\quad - (V_{\text{mag}}^+(\Delta k) - V_{\text{mag}}^-(\Delta k)) \sin \phi \sin \alpha], \\ \frac{1}{\tau_{\text{mag}}^A} &= \frac{\pi}{2\tau_F^m} (V_{\text{mag}}^+(\Delta k) - V_{\text{mag}}^-(\Delta k)) \cos \phi \cos \alpha, \end{aligned} \quad (\text{D2})$$

where the superscripts ‘‘A’’ (‘‘S’’) in τ_{mag}^A (τ_{mag}^S) refer to antisymmetry (symmetry), respectively. $1/\tau_{\text{mag}}^S$ ($1/\tau_{\text{mag}}^A$) gives the symmetry (antisymmetry) part of $1/\tau_{\text{mag}}$ when reversing k_x , respectively, namely, $1/\tau_{\text{mag}}^S(k_x, k_y) = 1/\tau_{\text{mag}}^S(-k_x, k_y)$ and $1/\tau_{\text{mag}}^A(k_x, k_y) = -1/\tau_{\text{mag}}^A(-k_x, k_y)$. Exploiting the parity of Table I, one can find that the term in brackets in Eq. (9) is an odd function of k_x ($\propto \cos \phi$). Therefore, only the antisymmetric part of $1/\tau_{\text{mag}}$ gives finite value to $a_{xx, \text{mag}}^{(2)}$, namely, USE induced by the asymmetry magnon scattering arising from $1/\tau_{\text{mag}}^A$.

The $\cos \phi$ dependence of $1/\tau_{\text{mag}}^A$ [Eq. (D2)] gives rise to cosine dependence on magnetization angle, namely, only the m_y ($\propto \cos \phi$) part of magnetization has a contribution to the unidirectional Seebeck effect. The m_x ($\propto \sin \phi$) part of the magnetization induces the symmetric magnon scattering [$1/\tau_{\text{mag}}^S$], which cannot lead to the antisymmetric contribution in the Seebeck effect when reversing the temperature gradient.

Figure 4(a) shows the variation of $1/\tau_{\text{mag}}$ with α for different magnetization orientation (i.e., ϕ). One can identify that $1/\tau_{\text{mag}}$ would be expressed as the function of $(\sin \alpha, \cos \alpha)$ [given in Eqs. (D1) and (D2)]. When increasing ϕ , the whole curve will shift towards lower α . The parities of $1/\tau_{\text{mag}}$ are strongly influenced by the magnetization orientation. The

absence of even properties in magnon relaxation time guarantees the existence of a unidirectional Seebeck effect. From Fig. 4(a), one can observe that only when the magnetization is aligned to the x direction [i.e., $\phi = \pi/2$ or $\phi = 3\pi/2$

(not shown) is $1/\tau_{\text{mag}}$ symmetric with respect to the mirror plane of $k_y - k_z$ ($\alpha = 90^\circ, 180^\circ$), namely, the presence of even properties about k_x . Thus, when magnetic field is not aligned in the x direction, the proposed effect would be observed.

-
- [1] M. Z. Hasan and C. L. Kane, *Rev. Mod. Phys.* **82**, 3045 (2010).
- [2] X.-L. Qi and S. C. Zhang, *Rev. Mod. Phys.* **83**, 1057 (2011).
- [3] L. Fu and C. L. Kane, *Phys. Rev. Lett.* **100**, 096407 (2008).
- [4] X.-L. Qi, R. Li, J. Zhang, and C. S. Zhang, *Science* **323**, 1184 (2009).
- [5] R. Yu, W. Zhang, H.-J. Zhang, S.-C. Zhang, X. Dai, and Z. Fang, *Science* **329**, 61 (2010).
- [6] R. Yoshimi, A. Tsukazaki, Y. Kozuka, J. Falson, K. S. Takahashi, J. G. Checkelsky, N. Nagaosa, M. Kawasaki, and Y. Tokura, *Nat. Commun.* **6**, 6627 (2015).
- [7] S. A. Wolf, D. D. Awschalom, R. A. Buhrman, J. M. Daughton, S. V. Molnár, M. L. Roukes, A. Y. Chtchelanova, and D. M. Treger, *Science* **294**, 1488 (2001).
- [8] A. Fert, *Rev. Mod. Phys.* **80**, 1517 (2008).
- [9] S. R. Boona, R. C. Myers, and J. P. Heremans, *Energy Environ. Sci.* **7**, 885 (2014).
- [10] G. E. W. Bauer, E. Saitoh, and B. J. V. Wees, *Nat. Mater.* **11**, 391 (2012).
- [11] X.-Q. Yu, Z.-G. Zhu, G. Su, and A.-P. Jauho, *Phys. Rev. Lett.* **115**, 246601 (2015).
- [12] X.-Q. Yu, Z.-G. Zhu, G. Su, and A.-P. Jauho, *Phys. Rev. Appl.* **8**, 054038 (2017).
- [13] C.-Z. Chang, J. Zhang, X. Feng, J. Shen, Z. Zhang, M. Guo, K. Li, Y. Ou, P. Wei, and L.-L. Wang *et al.*, *Science* **340**, 167 (2013).
- [14] K. Yasuda, A. Tsukazaki, R. Yoshimi, K. Kondou, K. S. Takahashi, Y. Otani, M. Kawasaki, and Y. Tokura, *Phys. Rev. Lett.* **119**, 137204 (2017).
- [15] C. O. Avci, K. Garello, A. Ghosh, M. Gabureac, S. F. Alvarado, and P. Gambardella, *Nat. Phys.* **11**, 570 (2015).
- [16] C. O. Avci, K. Garello, J. Mendil, A. Ghosh, N. Blasakis, M. Gabureac, M. Trassin, M. Fiebig, and P. Gambardella, *App. Phys. Lett.* **107**, 192405 (2015).
- [17] S. Langenfeld, V. Tshitoyan, Z. Fang, A. Wells, T. A. Moore, and A. J. Ferguson, *Appl. Phys. Lett.* **108**, 192402 (2016).
- [18] K. Yasuda, A. Tsukazaki, R. Yoshimi, K. S. Takahashi, M. Kawasaki, and Y. Tokura, *Phys. Rev. Lett.* **117**, 127202 (2016).
- [19] Y. Fan, P. Upadhyaya, X. Kou, M. Lang, S. Takei, Z. Wang, J. Tang, L. He, L.-T. Chang, M. Montazeri *et al.*, *Nat. Mater.* **13**, 699 (2014).
- [20] R. Yoshimi, K. Yasuda, A. Tsukazaki, K. S. Takahashi, N. Nagaosa, M. Kawasaki, and Y. Tokura, *Nat. Commun.* **6**, 8530 (2015).
- [21] K. Yasuda, R. Wakatsuki, T. Morimoto, R. Yoshimi, A. Tsukazaki, K. S. Takahashi, M. Ezawa, M. Kawasaki, N. Nagaosa, and Y. Tokura, *Nat. Phys.* **12**, 555 (2016).
- [22] J. Zhang, C.-Z. Chang, Z. Zhang, J. Wen, X. Fang, K. Li, M. Liu, K. He, L. Wang, X. Chen *et al.*, *Nat. Commun.* **2**, 574 (2011).
- [23] C. Z. Chang, J. Zhang, M. Liu, Z. Zhang, X. Feng, K. Li, L.-L. Wang, X. Chen, X. Dai, Z. Fang *et al.*, *Adv. Mater.* **25**, 1065 (2013).
- [24] G. D. Manhan, *Many Particle Physics*, 3rd ed. (Kluwer, New York, 2000).
- [25] X.-Q. Yu, Z.-G. Zhu, J.-S. You, T. Low, and G. Su, *Phys. Rev. B* **99**, 201410(R) (2019).
- [26] R. Yoshimi, A. Tsukazaki, K. Kikutake, J. G. Checkelsky, K. S. Takahashi, and Y. Tokura, *Nat. Mater.* **13**, 253 (2014).
- [27] Q. Liu, C.-X. Liu, C. Xu, X.-L. Qi, and S.-C. Zhang, *Phys. Rev. Lett.* **102**, 156603 (2009).
- [28] G. V. Skrotskii and L. V. Kurbatov, *Ferromagnetic Resonance* (Pergamon, New York, 1966).
- [29] Y. Onose, T. Ideue, H. Katsura, Y. Shiomi, N. Nagaosa, and Y. Tokura, *Science* **329**, 297 (2010).
- [30] K. Uchida, S. Takahashi, K. Harii, J. Ieda, W. Koshihae, K. Ando, S. Maekawa, and E. Saitoh, *Nature (London)* **455**, 778 (2008).
- [31] J. M. Ziman, *Electrons and Phonons: The Theory of Transport Phenomena in Solids* (Oxford University Press, New York, 1960).